

High Temperature Study on $\text{Er}_2\text{Ti}_2\text{O}_7$ Single Crystal

K. VLÁŠKOVÁ*, B. VONDRÁČKOVÁ, S. DANIŠ AND M. KLICPERA

Charles University, Faculty of Mathematics and Physics, Department of Condensed Matter Physics,
Ke Karlovu 5, 12116 Prague 2, Czech Republic

We present high temperature thermodynamical properties of a newly prepared $\text{Er}_2\text{Ti}_2\text{O}_7$ single crystal investigated by means of dilatometry and differential scanning calorimetry measurements. Measured data are dominated by a wide anomaly between 1250 K and 1540 K. The high-temperature powder X-ray diffraction experiment subsequently demonstrates the anomaly to be related to changes within the pyrochlore lattice, however, preserving the crystal symmetry in the whole temperature range.

DOI: [10.12693/APhysPolA.137.753](https://doi.org/10.12693/APhysPolA.137.753)PACS/topics: $\text{Er}_2\text{Ti}_2\text{O}_7$, DSC, dilatometry, X-ray diffraction, structure stability

1. Introduction

$\text{Er}_2\text{Ti}_2\text{O}_7$ belongs to the large family of $\text{A}_2\text{B}_2\text{O}_7$ oxides (A stays for the rare-earth element and B for transition metal or main *p*-block metal ion) that is isostructural with pyrochlore ($\text{Na,Ca}_2\text{Nb}_2\text{O}_6(\text{Oh,F})$; space group *Fd-3m*, No. 227. This family of compounds stays in the foreground of scientific interest mainly for its uncommon and frequently exotic low-temperature electronic properties including spin-ice state, spin-glass state, or magnetic monopole excitations. Such exotic electronic states origin mainly in magnetic cation on A and/or B site being a subject to a strong frustration: A and B cations (16*c* and 16*d* Wyckoff positions with $-3m$ point symmetry) form a net of mutually interpenetrating corner sharing tetrahedra in pyrochlore lattice, which represents thus a canonical example of geometrically frustrated structure. Oxygen anions at 8*a* and 48*f* Wyckoff sites form the 8- and 6-coordinate cages around A and B ions. As the cube and octahedron are unprotected by symmetry — it is formed by two crystallographic positions — it is usually deformed depending on the atomic size of A/B cations [1]. The change of local environment of magnetic cations, of course, plays crucial role in formation of physical properties of $\text{A}_2\text{B}_2\text{O}_7$, even though the lattice symmetry is preserved. The crystal structure of $\text{A}_2\text{B}_2\text{O}_7$ is governed mainly by the ratio between ionic radii of A and B cations, r_A/r_B . Depending on this ratio, the $\text{A}_2\text{B}_2\text{O}_7$ oxides can be generally grouped into three structure types, namely (i) defect fluorite ($r_A/r_B < 1.48$), (ii) pyrochlore ($1.48 < r_A/r_B < 1.78$), and (iii) perovskite ($r_A/r_B > 1.78$) [2].

The structural form of $\text{A}_2\text{B}_2\text{O}_7$ with r_A/r_B lying at the border line of structure stability strongly depends on the preparation conditions involving the size of crystallites and/or the preparation temperature. The complex study of hafnate family shows the occurrence of all stable defect fluorite structure, stable pyrochlore structure

and amorphous phase at room temperature and ambient pressure for the same $\text{A}_2\text{Hf}_2\text{O}_7$ compound depending solely on annealing temperature [3]. The lower annealing temperature determines the defect fluorite structure, whereas annealing the sample at elevated temperatures leads to the ordered pyrochlore structure. Temperature (> 1800 K) induced an order to disorder transition from a pyrochlore to a defect fluorite structure is observed in $\text{A}_2\text{Zr}_2\text{O}_7$ with $A = \text{Nd-Gd}$ [4]. Zirconates with A being heavy rare-earth element crystallize in defect fluorite structure, have been studied mainly from the view point of structure stability under extreme conditions [5, 6]. The stability of the structure depends mainly on the A/B ion intersite exchange energy [5] and on the energy of Frenkel anion oxygen pairs [7]. Changing the internal or external conditions, such as chemical doping, temperature of sample preparation, external pressure or irradiation of the sample, can lead to structural transitions between above listed structures [7–9].

Focusing on the rare-earth titanates, $\text{A}_2\text{Ti}_2\text{O}_7$ with $A = \text{La-Nd}$ adopt perovskite structure, whereas titanates with lower r_A/r_B ratio crystallize in a pyrochlore structure. The previous studies on $\text{Er}_2\text{Ti}_2\text{O}_7$ [10, 11] proved that the pyrochlore structure is stable up to high temperature (1273 K). Surprisingly, our data measured on newly-prepared high-quality single crystal showed a clear anomaly in temperature development of thermodynamic properties, as well as change of the lattice parameter at high temperature (between 1250 K and 1540 K).

2. Experimental results and discussion

A single crystal $\text{Er}_2\text{Ti}_2\text{O}_7$ was prepared by the floating zone technique from a stoichiometric mixture of starting oxides Er_2O_3 and TiO_2 . Contrary to previous studies [10, 12], where a pre-reacted polycrystal was used as a precursor, our single crystal preparation was more direct and clean. The use of initial oxides mixture, instead of $\text{Er}_2\text{Ti}_2\text{O}_7$ polycrystalline precursor, allows to minimize the composition deviation (and contamination) caused by repeated heating-cooling cycles with intermediate grindings of the mixture [13, 14]. The investigation of sample

*corresponding author; e-mail: kristinavl@seznam.cz

quality (X-ray diffraction, energy dispersive X-ray analysis, neutron diffraction) and its low temperature bulk properties (magnetization, specific heat), brought the results well comparable (almost identical) with previously published data on single crystals prepared from 227 polycrystalline precursor [14]. The present study focus on the high-temperature properties of our $\text{Er}_2\text{Ti}_2\text{O}_7$ single crystal, and more specifically on its crystal structure stability.

The dilatometry measurement with a heating rate of 3 K/min under helium protective and thermally conducting atmosphere was carried out using NETZCH DIL 402 C instrument. The differential scanning calorimetry (DSC) analysis was performed on a SETSYS Evolution 24 instrument from SETARAM Instrumentation with a heating rate of 10 K/min also in He atmosphere. The respective properties were investigated in the same temperature range from 300 K to 1630 K. The high temperature powder X-ray diffraction experiment was performed using X'Pert Pro PANalytical with copper K_α radiation ($\lambda = 1.5406 \text{ \AA}$). The sample was placed directly on the platinum plate holder, which served as an ohmic heater simultaneously. Further, heating power was supplied by Pt radiation heater placed a few cm from the sample. Heating rate of 5 K/min was used. Thermal equilibrium for individual thermal scans was reached within ≈ 15 min of temperature stabilization before each measurement of diffraction patterns. Diffraction patterns were processed using FullProf package.

The differential scanning calorimetry measurement revealed a smooth development of heat flow with increasing temperature up to 1250 K, see Fig. 1a. At higher temperature a clear, although broad, anomaly develops (up to 1540 K). On cooling a corresponding anomaly manifests itself on the same temperature interval. Although we take into account the heating/cooling rate of 10 K/min for our DSC experiment, the anomaly is very broad pointing out to a gradual change of phase/lattice. Second (subsequent) DSC measurement reproduced the main features of the first heating/cooling cycle, except the anomaly on heating was significantly less pronounced. No change of sample morphology was observed after the measurement. The measurement to even higher temperature is desirable, however, not achievable by our instrument.

An anomaly at high temperature is followed also on temperature evolution of relative elongation of the sample measured along [100] and [110] crystallographic directions. Dilatometry data are shown in Fig. 1b. We note that the temperature of the anomaly (on heating and cooling) is shifted to higher temperature compared to DSC data due to the significantly smaller heating/cooling rate of 3 K/min (allowing the sample to follow temperature changes closely). The data measured along both crystallographic directions are consistent exhibiting the anomalies at the same temperature. Thermal expansion along [110] direction is larger (factor of square root of two) than that measured along [100]. This is

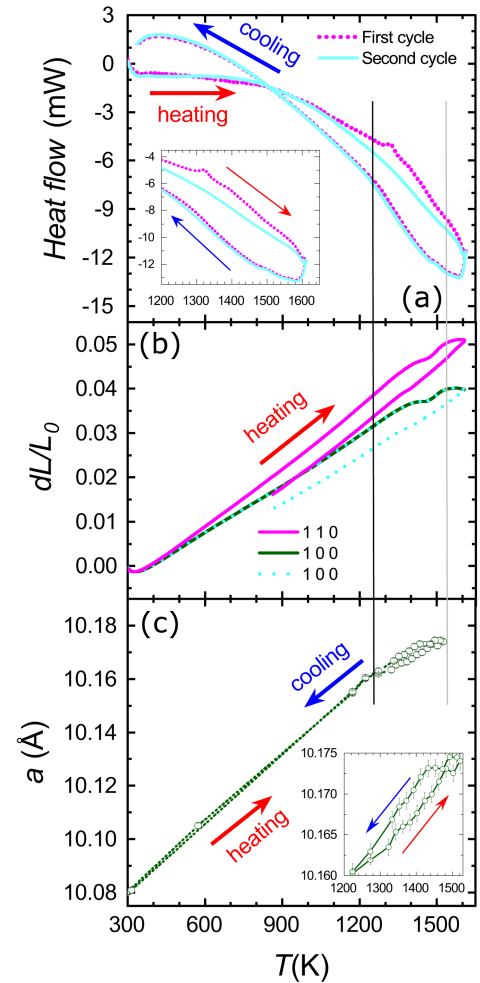


Fig. 1. Temperature evolution of thermodynamic properties and lattice parameter a in $\text{Er}_2\text{Ti}_2\text{O}_7$ single crystal. (a) DSC data — two heating/cooling cycles were measured on the same sample. (b) Dilatometry measurement along [100] and [110] crystallographic direction. (c) Lattice parameter a refined using model pyrochlore structure. Zoomed anomaly/hysteresis of properties is shown in inset.

expected as [110] is the plane diagonal. Two subsequent measurements along [100] direction differ only negligibly. Considering different heating/cooling rate in DSC and dilatometry experiments the respective data are well in agreement.

The high temperature X-ray diffraction experiment confirmed the results of DSC and dilatometry measurements showing a clear evolution of diffraction patterns with temperature. The temperature development of X-ray patterns (Bragg reflections) measured at selected temperatures is plotted in Fig. 2. A slight change of peak position (lattice parameter) with temperature is observed only up to ~ 1200 K. An expected thermal expansion of the material is followed (see also Fig. 1c). At higher temperatures a change of diffraction patterns (both intensity and position of peaks) is manifested. This structural change is however not related to the change of

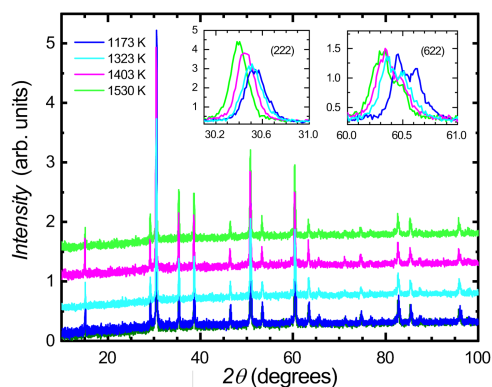


Fig. 2. X-ray diffraction patterns. The evolution of peaks positions and intensities at selected temperatures (outside, and inside of 1250 K– 1540 K interval) are shown.

crystal structure (or at least the change of its symmetry), since the diffraction patterns are described by a pyrochlore structure in the whole temperature range. No additional Bragg reflections appear at high temperature. Temperature development of lattice parameter a during cooling/heating cycle is shown in Fig. 1c. Interestingly, a hysteretic behavior of a under heating/cooling regime is followed. Although the difference of the lattice parameter is relatively small, it exceeds the magnitude of the error bars and shows a clear tendency. The temperature range of hysteresis corresponds well to anomalies in DSC and dilatometry data.

The intensity on a number of reflections significantly increases within the temperature interval 1250–1540 K (see Fig. 2). The intensity change can be generally ascribed to thermal fluctuations of individual ions on their respective positions (atomic displacement — Debye-Waller factor). For crystallographic reasons only Er and Ti planes contribute to the intensity of the reflection of the crystallographic plane (222) in inset of Fig. 2. On the other hand, the intensity on, e.g. (622) reflection, is formed also by oxygen sites, and no clear change of the intensity is followed with increasing temperature on this reflection. Such observation suggests a more significant change of structural parameters of Er/Ti cations compared to oxygen anions within the unit cell. The pyrochlore structure however leaves only 48 f oxygen site free ($x, 1/8, 1/8$). Surprisingly, the x parameter ($x = 0.326(2)$) is independent on temperature, i.e., it remains constant within the experimental error. Nevertheless, a subtle turn of oxygen octahedra, preserving average (global) crystal symmetry, cannot be ruled out. To prove such an assumption both more advanced X-ray/neutron diffraction techniques and higher temperature experiments are highly desirable.

3. Conclusions

$\text{Er}_2\text{Ti}_2\text{O}_7$ single crystal was studied at high temperatures using DSC, dilatometry and powder X-ray diffraction techniques. The broad anomaly in both DSC and

dilatometry data was followed on temperature interval 1250–1540 K. The observed anomaly is connected to the hysteretic behavior of lattice parameter a as determined by high temperature X-ray diffraction. The average (global) pyrochlore structure is preserved up to highest temperature. The observed anomalies can be ascribed to a subtle turn of oxygen octahedra in pyrochlore lattice.

Acknowledgments

This work was supported by the Czech Science Foundation under Grant No. 18-09375Y. The work of K.V. was further supported by GAUK Project No. 558218. The preparation, characterization and measurement of bulk physical properties on $\text{Er}_2\text{Zr}_2\text{O}_7$ were performed in MGML, (<http://mgml.eu/>), which was supported within the program of Czech Research Infrastructures (project No. LM2018096).

References

- [1] M.A. Subramanian, G. Aravamudan, G.V. Subba Rao, *Prog. Sol. Stat. Chem.* **15**, 55 (1983).
- [2] S.J. Patwe, V. Katari, N.P. Salke, S.K. Deshpande, R. Rao, M.K. Gupta, R. Mittal, S.N. Achary, A.K. Tyagi, *J. Mater. Chem. C* **3**, 4570 (2015).
- [3] V.V. Popov, A.P. Menushenkov, A.A. Yaroslavtsev, Y.V. Zubavichus, B.R. Gaynanov, A.A. Yastrebtshev, D.S. Leshchev R.V. Chernikov, *J. Alloys Comp.* **689**, 669 (2016).
- [4] M. Rushton, R. Grimes, C.R. Stanek, S. Owens, *J. Mater. Res.* **19**, 1603 (2004).
- [5] K.E. Sickafus, L. Minervini, R.W. Grimes, J.A. Valdez, M. Ishimaru, F. Li, K.J. McClellan, T. Hartmann, *Science* **289**, 748 (2000).
- [6] D.W. Shoesmith, M. Razdan, *J. Electrochem. Soc.* **161**, 105 (2014).
- [7] F.X. Zhang, M. Lang, R.C. Ewing, *Appl. Phys. Lett.* **106**, 191902 (2015).
- [8] R. Clements, J.R. Hester, B.J. Kennedy, Ch.D. Ling, A.P.J. Stampfl, *J. Sol. State Chem.* **184**, 2108 (2011).
- [9] H. Li, Q. Tao, N. Li, R. Tang, Y. Zhao, H. Zhu, P. Zhu, X. Wang, *J. Alloys Comp.* **660**, 446 (2016).
- [10] Q. Wang, A. Ghasemi, A. Scheie, S.M. Koohpayeh, *Cryst. Eng. Comm.* **21** (4), 703 (2019).
- [11] J.M. Farmer, L.A. Boatner, B.C. Chakoumakos, M.H. Du, M.J. Lance, C.J. Rawn, J.C. Bryan, *J. Alloys Comp.* **605**, 63 (2014).
- [12] Q. J. Li, L. M. Xu, C. Fan, F.B. Zhang, Y.Y. Lu, B. Ni, Z.Y. Zhao, X.F. Sun, *J. Cryst. Growth* **377**, 96 (2013).
- [13] K. Vlášková, R.H. Colman, P. Proschek, J. Čapek, M. Klicpera, *Phys. Rev. B* **100**, 214405 (2019).
- [14] K. Vlášková, P. Proschek, J. Pospíšil, M. Klicpera, under review in *J. Crystal. Growth*.